

The BiomolBiomed publishes an "Advanced Online" manuscript format as a free service to authors in order to expedite the dissemination of scientific findings to the research community as soon as possible after acceptance following peer review and corresponding modification (where appropriate). An "Advanced Online" manuscript is published online prior to copyediting, formatting for publication and author proofreading, but is nonetheless fully citable through its Digital Object Identifier (doi®). Nevertheless, this "Advanced Online" version is NOT the final version of the manuscript. When the final version of this paper is published within a definitive issue of the journal with copyediting, full pagination, etc., the new final version will be accessible through the same doi and this "Advanced Online" version of the paper will disappear.

RESEARCH ARTICLE

Filippova et al: LncRNA and co-methylation in breast CA

LncRNA interactomes and co-methylation in breast cancer regulation

Elena A. Filippova^{1*}, Irina V Pronina², Svetlana S Lukina¹, Alexey M Burdenny¹,
Tatiana P Kazubskaya³, Vitaly I Loginov¹ and Eleonora A Braga¹

¹Institute of General Pathology and Pathophysiology, Moscow, Russia

²N.M. Emanuel Institute of Biochemical Physics, Russian Academy of Science, Moscow, Russia

³N.N. Blokhin National Medical Research Center of Oncology, the Ministry of Health of Russia, Moscow, Russia

*Correspondence to **Elena Filippova**: p.lenyxa@yandex.ru

DOI: <https://doi.org/10.17305/bb.2025.12333>

ABSTRACT

Breast cancer is the most commonly diagnosed malignancy in women. Despite advances in diagnostics and treatment, the key molecular mechanisms underlying its development remain incompletely understood. This study aimed to identify novel lncRNA–miRNA–mRNA regulatory networks potentially involved in breast cancer–associated signaling pathways. Using an RT² lncRNA PCR Array and bioinformatic analysis, we identified seven differentially expressed (DE) lncRNAs. Four of these—ADAMTS9-AS2, HAND2-AS1, HOTAIRM1, and MEG3—were prioritized through integrative evaluation. qPCR confirmed their downregulation and aberrant methylation in breast tumor samples. We observed significant positive expression correlations between the pairs ADAMTS9-AS2–MEG3, HAND2-AS1–MEG3, and HOTAIRM1–MEG3, as well as co-methylation among ADAMTS9-AS2–HAND2-AS1, ADAMTS9-AS2–HOTAIRM1, HAND2-AS1–MEG3, and HAND2-AS1–HOTAIRM1, suggesting coordinated regulation. These findings are consistent with data from GEPIA 2.0. Bioinformatic prediction identified TCF7L2 as a common target gene of these lncRNAs, which is involved in the Wnt, Hippo, and MAPK signaling pathways. We also identified several miRNAs interacting with ADAMTS9-AS2. In a cohort of 50 tumor samples, we confirmed inverse associations between ADAMTS9-AS2 expression and levels of miR-106a-5p ($r_s = -0.46, p = 0.03$) and miR-17-5p ($r_s = -0.41, p = 0.04$). Collectively, these findings reveal novel co-regulated lncRNA–miRNA axes and suggest their involvement in key signaling networks in breast cancer, providing a foundation for future functional studies and potential therapeutic targeting.

Keywords: lncRNA PCR Array; lncRNAs co-expression; lncRNA genes co-methylation; ADAMTS9-AS2; lncRNA–miRNA–mRNA regulatory axes.

INTRODUCTION

Breast cancer (BC) has been the most common type of cancer found in women for many years [1]. Despite the rapid development of modern new postgenomic technologies that allow for early diagnosis of the disease and significant improvements in the treatment protocols, the mortality rate remains high. The development of metastases is the leading cause of high mortality rate in breast cancer patients [2]. Given the remarkable heterogeneity of breast tumors, standard treatment protocols may not be sufficiently effective; therefore, an in-depth study of the mechanisms underlying breast cancer development and progression is necessary. Identifying the key regulators of signaling pathways that lead to breast cancer progression and the development of metastases will allow us to make a significant progress in searching for the most effective personalized therapy, and increase the survival rate of patients with breast cancer.

Due to significant advances in genome-wide technologies over the past decade, we now have a profound understanding of the key role of non-coding RNAs (ncRNAs) in regulating the genes involved in every step of tumor development and progression, as well as the involvement of ncRNAs in relapse and drug resistance [3-5.] Recent research indicates the enormous potential of ncRNAs, namely their two main classes: long non-coding RNAs (lncRNAs) and microRNAs (miRNAs) as diagnostic/prognostic biomarkers, as well as therapeutic targets for breast cancer [6, 7]. lncRNAs are non-protein-coding RNAs that are about 200 nucleotides long and play a dynamic regulatory role in both normal and pathological processes, including carcinogenesis [5]. miRNAs are evolutionarily conserved single-stranded RNAs which are 17–25 nucleotides long, the 5'-site bases of which are bound to miRNA response elements (MREs) which are approximately 7 nt long in the 3'-UTR of their target mRNAs in the RNA-induced silencing complex (RISC) [8]. Moreover, lncRNAs and miRNAs regulate gene expression through interactions in the lncRNA-miRNA-mRNA regulatory axes, so it is relevant to study both the regulatory networks of lncRNAs and miRNAs and their overlapping points. The functional role of lncRNA and miRNA regulatory networks was established for the development and progression of some forms of cancer [9]. Depending on its composition, the lncRNA-miRNA-mRNA axis can exhibit both tumor-suppressive and oncogenic properties in a certain type of cancer. lncRNAs are considered to act as competing endogenous RNAs that bind miRNAs based on the same mechanism as mRNAs, preventing miRNAs from binding to the target mRNA and thereby reducing mRNA repression [10]. There are also alternative mechanisms for regulating gene expression by ncRNAs. lncRNAs can be precursors of

microRNAs, which undergo processing to form miRNAs from exons or introns. miRNAs can also regulate lncRNAs by binding to them and further degrading lncRNAs in the RISC complex. lncRNAs and miRNAs can also compete for mRNA binding sites. lncRNAs can mask the miRNA binding site, preventing the degradation of target mRNAs [11]. Scrutinizing the lncRNA-miRNA interactions provides for targeted therapy. The search for and validation of new lncRNA-miRNA-mRNA axes in breast cancer will enable the development of precise strategies to specifically inhibit the expression of proteins contributing to breast cancer progression. As both lncRNAs and miRNAs can function as tumor suppressors and oncogenes, and even the same lncRNA/miRNA can play a dual role in the same type of cancer, the use of the lncRNA-miRNA axis as targeted therapy seems to be the most effective solution potentially reducing the likelihood of off-target effects.

This work aimed to identify new lncRNA-miRNA-mRNA regulatory axes in breast cancer. In addition, as we have recently noted it for miRNA genes in ovarian cancer [12], co-methylation is often found among the hypermethylated non-coding RNA genes. In this regard, another goal of this work was to identify cross-regulation of lncRNAs in breast cancer through methylation of their genes.

MATERIALS AND METHODS

Bioinformatic analysis

Using the Gene Expression Omnibus (GEO) database, differentially expressed lncRNAs corresponding to “breast cancer,” “gene expression,” and “tissues” were screened for in the public datasets. As a result, the GSE22820 dataset (from 176 primary breast cancer patients and 10 normal breast samples), which contained the genes differentially expressed in breast tumor tissues and adjacent normal tissues, was selected for further analysis. We used GEO2R to analyze the differentially expressed genes in the dataset and selected the genes based on the following criteria: $\log_{2}FC \geq \pm 1$ and $P < 0.05$. To compare the data established experimentally using the RT² lncRNA PCR Array (Qiagen) [13] and the bioinformatic analysis, and to search for a common set of overlapping differentially expressed genes, we used the source at <http://bioinformatics.psb.ugent.be/webtools/Venn/>. To select epithelial to mesenchymal transition-associated lncRNAs from a preliminary set of genes, the GeneCard database (<https://www.genecards.org/>) was used; the search was performed using the keyword “EMT”. To compare and verify the results, we analyzed the GEPIA 2.0 database ([4](http://gepia.cancer-</p></div><div data-bbox=)

pku.cn/). To search for and select miRNAs that potentially interact with the studied lncRNAs, the DIANA-LncBase v3 (<https://diana.e-ce.uth.gr/lncbasev3>) and RNAInter (<http://www.rnainter.org/>) databases were used. The NcPath (<http://ncpath.pianlab.cn/>) and miRPath v.3 (<https://dianalab.e-ce.uth.gr/html/mirpathv3/index.php?r=mirpath>) databases were used for the search and analysis of common signaling pathways and biological processes in which the non-coding RNAs are involved. To verify the possibility of interaction between lncRNA and mRNA, the LncRRISearch web server was used (<http://rtools.cbrc.jp/LncRRISearch/>); to predict the interaction between microRNA and mRNA, the miRWalk 2.0 database was used (<http://mirwalk.umm.uni-heidelberg.de/>).

Collection of samples

127 paired (tumor/adjacent histologically normal breast tissue) breast cancer samples were collected and morphologically characterized in the Department of Tumor Pathomorphology of N.N. Blokhin National Medical Research Center of Oncology based on the WHO classification [14]. The diagnosis was made on the basis of histological findings. The clinical and morphological characteristics of 127 breast cancer samples are presented in Table 1.

Criteria for inclusion in the study were as follows: 1) a verified diagnosis of breast cancer; 2) a clinical and histological description of the samples obtained (stage, degree of differentiation, tumor size, presence or absence of lymphnode metastases. Exclusion criteria: 1) chemotherapy or radiation therapy; 2) severe chronic infections; 3) severe concomitant somatic pathology (chronic diseases); 4) tumor location other than the breast (after additional histological analysis). The work was conducted in compliance with the principles of voluntariness and confidentiality in accordance with the Declaration of Helsinki of the World Medical Association [15].

To select samples with a high content of tumor cells (at least 70%), additional histological analysis of microsections (3-5 μm) stained with hematoxylin and eosin was performed. Tissue samples were stored at $-70\text{ }^{\circ}\text{C}$. The tissue frozen in liquid nitrogen was crushed using the TissueRuptor® II homogenizer (QIAGEN, Hilden, Germany).

Extraction of total DNA and RNA, assessment of the purity of preparations

High-molecular-weight DNA was isolated using standard phenol-chloroform extraction. The DNA concentration was determined based on optical density at a wavelength of 260 nm, and the degree of DNA purification was determined based on the spectrum at the wavelengths from

230 to 320 nm on the NanoDrop ND-1000 spectrophotometer (Thermo Fisher Scientific, Wilmington, DE, USA). DNA quality was determined by conducting electrophoresis on 0.8% agarose gel using the Sub-Cell GT Horizontal Electrophoresis System (Bio-Rad, Hercules, CA, USA), followed by gel imaging with the Gel Doc XR+ Gel Documentation System (Bio-Rad). DNA was stored at -20°C.

Total RNA from paired breast tissue samples (tumor/adjacent histologically normal breast tissue) was extracted using ExtractRNA #BC032 reagent (Evrogen, Moscow, Russia). RNA samples were treated with RQ1 RNase-Free DNase (Promega, CA, USA) in accordance with the manufacturer's protocol. The RNA concentration was determined based on optical density at a wavelength of 260 nm on the NanoDrop ND-1000 spectrophotometer (Thermo Fisher Scientific) with an additional assessment of the degree of purification of the total RNA preparation based on the absorption ratio at wavelengths of 260 and 280 nm and the shape of the absorption spectrum curve at wavelengths 230-320 nm. RNA was stored at -20°C.

Assessment of the differential expression of lncRNAs in clinical samples using the RT²

lncRNA PCR Array

Using the RT² lncRNA PCR Array #LAHS-002Z (QIAGEN Sciences, Frederick, MD, USA), the differential expression of 84 lncRNAs in breast cancer samples was analyzed. Each cataloged lncRNA RT² PCR array contains a list of genes targeted at a specific signaling pathway, as well as five housekeeping genes. In addition, each array contains a panel of proprietary "controls" to monitor genomic DNA contamination, as well as first-strand synthesis and real-time PCR efficiency. Reverse transcription was carried out using RT² First Strand Kit (QIAGEN Sciences). qPCR was carried out using RT² SYBR® Green qPCR Mastermix (Cat. # 330529, QIAGEN Sciences). CT values were exported to an Excel file to create a table of CT values. That table was then uploaded to the data analysis portal at <http://www.qiagen.com/geneglobe>. The samples were assigned to the control and test groups. CT values were normalized based on manual selection of reference genes. The data analysis portal calculates the rate of change/regulation using the "ΔΔCT" method.

Assessment of the gene methylation and gene expression levels in clinical samples by

Real-Time PCR

The level of lncRNA genes methylation was analyzed using bisulfite conversion of DNA and quantitative methyl-specific PCR with real-time detection (MS-qPCR), as described in [16].

Amplification was performed on the Bio-Rad CFX96 Real-Time PCR Detection System (Bio-Rad, CA, USA) using the qPCRmix-HS SYBR kit (Evrogen, Moscow, Russia) in accordance with the manufacturer's protocol. The oligonucleotide sequences and PCR conditions for the lncRNA genes ADAMTS9-AS2, HAND2-AS1, HOTAIRM1, MEG3, and the control gene ACTB1 are shown in Table 2. The commercial preparation Human Genomic DNA (#G1471; Promega, CA, USA) was used as controls for unmethylated alleles. The commercial preparation of CpG Methylated Human Genomic DNA (#SD1131; Thermo Fisher Scientific, DE, USA) was used as a positive control for 100% methylation.

Reverse transcription of total RNA was performed using the MMLV RT kit # SK021 (Evrogen). Quantitative PCR was performed on the Bio-Rad CFX96 Real-Time PCR Detection System amplifier (Bio-Rad) using the qPCRmix-HS SYBR kit (Evrogen). The primer sequences and PCR conditions for the lncRNAs ADAMTS9-AS2, HOTAIRM1, MEG3, HAND2-AS1, and the reference gene B2M are shown in Table 3. The data were analyzed using relative quantification based on the $\Delta\Delta C_t$ method [17]. The changes in lncRNA levels which were less than two times ($|\Delta\Delta C_t| \leq 2$) were considered as no changes. The PCR was performed in three technical replicates.

Reverse transcription of miRNA was performed using the TaqMan™ MicroRNA Reverse Transcription Kit (Thermo Fisher Scientific) with the total RNA amount of 6 ng/reaction. The PCR was performed using the TaqMan Fast Universal PCR MasterMix (Thermo Fisher Scientific) and Taq Man MicroRNA Assays (Thermo Fisher Scientific) kits for hsa-miR-106a (AssayID: 002169) and hsa-miR-17 (AssayID: 002308), reference RNAs: RNU6B (AssayID: 001093), RNU48 (AssayID: 001006). The PCR was performed using the Bio-Rad CFX96 Real-Time PCR Detection System thermal cycler (Bio-Rad).

Ethical statement

The study was conducted in accordance with the Declaration of Helsinki, and approved by the Ethics Committee of the Institute of General Pathology and Pathophysiology (protocol №1 03.03.2022; protocol №4 31.08.2023).

Statistical analysis

The results were analyzed in the R software environment. To assess the significance of differences between the studied groups, the non-parametric Mann–Whitney U test was used for independent samples. To assess the contribution of promoter CpG island methylation to the

regulation of lncRNA gene expression, we calculated $\Delta\beta$ (delta beta) values, representing the difference in methylation levels between tumor and paired normal tissues. The analysis of possible co-expressions was performed using the Spearman's correlation coefficient adjusted for the Benjamini-Hochberg multiple comparisons procedure. The differences were considered to be significant at $p \leq 0.05$.

RESULTS

Differential expression of lncRNAs in breast cancer: RT² PCR Array and bioinformatic screening

To comprehensively evaluate the role of long non-coding RNAs (lncRNAs) in breast cancer, we employed the RT² lncRNA PCR Array (QIAGEN Sciences) to assess the expression of 84 lncRNAs in 12 paired tumor and adjacent normal breast tissue samples. The initial screening results, which were previously reported at the 2nd International Electronic Conference on Biomedicine (2023) [13], revealed a statistically significant decrease in the expression level of 30 lncRNAs: ACTA2-AS1, ADAMTS9-AS2, BANCER, EMX2OS, H19, HAND2-AS1, HIF1A-AS1, HOTAIRM1, HOXA-AS2, JADRR, KRASP1, LINC00312, LINC00538, LINC01233, LSINCT5, LUCAT1, MEG3, MIR31HG, MIR7-3HG, NAMA, PCA3, PCGEM1, PTENP1, RMRP, SPRY4-IT1, TRERNA1, TSIX, TUSC7, WT1-AS, XIST, while the expression level of two lncRNAs (TERC, RPLP0) was significantly increased (Figure 1; Table S1).

To further reinforce the biological significance of our experimental findings, we conducted an in silico analysis using the GSE22820 dataset, comprising 176 breast carcinoma and 10 normal tissue samples, offers robust transcriptional profiling for identifying differentially expressed lncRNAs ($p < 0.05$, $|\log_2FC| > 1$) relevant to breast cancer. Despite limited clinical annotations, its large sample size and molecular diversity provide valuable insights into tumor heterogeneity and oncogenic pathways. Figure 2A presents a volcano plot of differentially expressed genes in the GSE22820 dataset. Overlapping the GEO2R-derived lncRNAs with our experimental data via Venn diagram analysis revealed seven commonly dysregulated candidates (*HOTAIRM1*, *HAND2-AS1*, *ADAMTS9-AS2*, *EMX2OS*, *WT1-AS*, *MIR31HG*, *MEG3*) (Figure 2B). Further, *EMX2OS*, *WT1-AS*, and *MIR31HG* were excluded based on non-significant differential expression ($p > 0.01$) between tumor and normal tissue in TCGA (BRCA) data. This additional filtering step using an independent dataset (TCGA BRCA) served as a

preliminary cross-test to improve the robustness of our approach. The remaining four lncRNAs were prioritized due to their biological and clinical relevance. Functional enrichment analysis revealed over 90 EMT and metastasis-associated biological processes linked to *MEG3*, while *HOTAIRM1* was implicated in three metastasis-related processes (GO:1904019, GO:1904035, GO:1904036). *HAND2-AS1* showed a significant association with overall survival, underscoring its prognostic potential. *ADAMTS9-AS2* was enriched in Hippo signaling and several EMT-related pathways (e.g., GO:0023061, GO:0002790, GO:0015833), highlighting a likely role in epigenetic regulation and tumor progression.

Expression and methylation analysis of lncRNAs and their regulatory interplay

We next evaluated the expression of the four candidate lncRNAs in 50 paired breast tumor and normal tissue samples, confirming significant downregulation for all 4 lncRNAs (*ADAMTS9-AS2*, *HAND2-AS1*, *HOTAIRM1*, *MEG3*) ($p < 0.001$) (Figure 3A). Considering promoter hypermethylation as a plausible epigenetic mechanism regulating gene expression, methylation-specific qPCR (MS-qPCR) was conducted on 127 breast cancer samples. The analysis revealed significant hypermethylation ($p < 0.05$) in the promoter regions of all four lncRNAs *ADAMTS9-AS2*, *HAND2-AS1*, *HOTAIRM1*, *MEG3* (Figure 3B). This suggests that promoter hypermethylation may contribute to the transcriptional silencing of these lncRNAs in breast cancer. Using a set of 50 paired samples with both methylation and expression data, Spearman's analysis revealed a strong negative correlation between promoter methylation ($\Delta\beta$) and *ADAMTS9-AS2* expression ($r_s = -0.67$; $p = 0.07$), suggesting a potential role of hypermethylation in its transcriptional silencing. This trend was further supported by integrative analyses using the MethMarkerDB database, contain data from the TCGA 450K methylation array and RNA-Seq, which helped to evaluate the correlation between gene expression levels and methylation of the gene itself or its associated differentially methylated regions (DMRs). These analyses consistently demonstrated a negative correlation between *ADAMTS9-AS2* methylation and expression in independent, larger cohorts. Together, these findings show that DNA methylation plays a regulatory role in modulating *ADAMTS9-AS2* expression. The correlation between methylation levels and *ADAMTS9-AS2* expression, identified through bioinformatic analysis and observed as a trend in a cohort of 50 samples, appears to be biologically meaningful; however, further validation is warranted in future studies, which may include expanding the sample size as well as employing in vitro models using demethylating agents such as 5-azacytidine.

Further stratified analysis demonstrated that promoter hypermethylation of HAND2-AS1, HOTAIRM1, and MEG3 was significantly elevated in samples from patients with advanced tumor stages, tumor size, and lymphnode metastases (Figures 3C, 3D), suggesting a potential link between lncRNA methylation and tumor progression.

Notably, analysis of MEG3 expression using the Kruskal–Wallis test revealed a significant variation across different immunohistochemical subtypes of breast cancer ($p = 0.014$), with the most pronounced differences observed between the Erb-B2 and Luminal B subtypes. These findings imply a possible association between MEG3 dysregulation and specific molecular subtypes of breast cancer. For the remaining lncRNAs, no significant associations with molecular subtypes, receptor status (ER, PR, HER2), or tumor grade were observed, suggesting their dysregulation may reflect general tumor progression rather than subtype-specific mechanisms.

Pairwise co-expression and co-methylation of lncRNAs in the regulation of common signaling pathways

Our experimental analyses revealed significant co-expression and co-methylation patterns among the long non-coding RNAs (lncRNAs) MEG3, HOTAIRM1, HAND2-AS1, and ADAMTS9-AS2, suggesting potential coordinated epigenetic regulation (Figure 4). Spearman's correlation analysis of expression levels revealed consistent positive associations between several lncRNA pairs, including MEG3–HOTAIRM1, MEG3–ADAMTS9-AS2, and MEG3–HAND2-AS1. These results were consistent with data obtained from the GEPIA 2.0 database, which compiles gene expression profiles from the TCGA BRCA cohort (comprising 1085 tumor and 112 normal breast tissue samples), reinforcing the reproducibility and robustness of our observations (Figure 4, Table 4).

In parallel, promoter methylation analysis using methylation-specific qPCR (MS-qPCR) demonstrated strong positive correlations in methylation levels across the same lncRNA pair, MEG3–HAND2-AS1, previously identified as co-expressed. In addition, co-methylation was also observed for the pairs ADAMTS9-AS2–HAND2-AS1, HAND2-AS1–HOTAIRM1, and ADAMTS9-AS2–HOTAIRM1, further supporting the hypothesis of shared epigenetic regulation among these lncRNAs in breast cancer. These co-methylation patterns were further supported by the expression correlations observed in GEPIA, implying potential synergistic epigenetic regulation of these transcripts (Figure 4, Table 4). Thus, the co-expression and co-

methylation patterns may point toward coordinated involvement in common molecular pathways.

To explore the potential biological relevance of these lncRNA interactions, we performed pathway enrichment analysis using the NcPath database, which integrates information from KEGG. This analysis revealed that the co-expressed and co-methylated lncRNAs are associated with seven critical cancer-related signaling pathways: Hippo, MAPK, Wnt, adherens junction, focal adhesion, PI3K-Akt, and mTOR. Notably, ADAMTS9-AS2, HOTAIRM1, and MEG3 were found to converge on a shared target—TCF7L2, a transcription factor implicated in Hippo, Wnt, and adherens junction pathways.

Further pathway mapping revealed that these lncRNAs also regulate several extracellular matrix (ECM)-related genes involved in metastasis and cell adhesion. For instance, HOTAIRM1 regulates THBS4, MEG3 regulates THBS1, and both ADAMTS9-AS2 and MEG3 share targets including ERBB4 (in MAPK and PI3K-Akt pathways), ITGA3 (in PI3K-Akt and focal adhesion), and WNT3 (in Hippo, mTOR, and Wnt pathways).

Together, our data suggest that MEG3, HOTAIRM1, HAND2-AS1, and ADAMTS9-AS2 may constitute a co-regulated epigenetic network involved in the modulation of signaling cascades that drive breast cancer progression.

Co-expression of miRNAs in common signaling pathways

To investigate the potential regulatory function of lncRNAs mediated by miRNAs, we conducted bioinformatic analysis to predict miRNAs that might interact with the four studied lncRNAs (ADAMTS9-AS2, HAND2-AS1, HOTAIRM1, and MEG3). Using well-established bioinformatic tools such as DIANA-LncBase and RNAInter, we identified miR-17-5p and miR-106a-5p as potential interactors of these lncRNAs. This suggests the formation of a functional lncRNA–miRNA regulatory axis that could be relevant to breast cancer progression. Public dataset analysis further highlighted the significant roles of miR-17-5p and miR-106a-5p in breast cancer, underlining their involvement in disease progression (Table 5).

In our experimental analysis, RT-qPCR of 50 paired breast tumor and normal tissue samples revealed a strong positive correlation between the expression levels of miR-17-5p and miR-106a-5p ($r_s = 0.78$; $p < 0.001$). This high co-expression suggests that these miRNAs likely act in a coordinated manner, playing an important role in breast cancer progression.

Furthermore, functional enrichment analysis performed using the miRPath v.3 database identified several key signaling pathways, including Hippo, MAPK, Wnt, adherens junction, and focal adhesion, that are shared between miR-17-5p and miR-106a-5p (Figure 5). Moreover,

these same pathways are included among those predicted for 4 lncRNAs according to KEGG data (previous chapter). These overlapping pathways suggest that both selected miRNAs and lncRNAs could be involved in similar regulatory networks. The co-expression patterns observed in our experimental data align with the bioinformatic predictions, supporting the hypothesis of common targets and pathways.

Determining the miRNA-lncRNA “axis” in the regulation of common signaling pathways in breast cancer

To identify potential miRNA-lncRNA regulatory pairs involved in common signaling pathways, we compared the expression levels of miR-106a-5p and miR-17-5p with the expression of 4 lncRNAs using Spearman’s correlation coefficient. A moderate negative correlation was observed between miR-106a-5p and ADAMTS9-AS2 ($r_s = -0.46$; $p = 0.03$), as well as between miR-17-5p and ADAMTS9-AS2 ($r_s = -0.41$; $p = 0.04$) (Figure 6).

GO and KEGG enrichment analyses (Figure 7) were performed individually for each miRNA and for ADAMTS9-AS2 to identify shared pathways and functional features. Notably, miR-17-5p was enriched in GO terms directly related to methylation processes (GO:0044027, GO:0141137), highlighting its potential involvement in the regulation of DNA methylation. Additionally, common pathways identified, including the Hippo signaling pathway, known to play a crucial role in metastasis, suggest that miR-17-5p, miR-106a-5p, and ADAMTS9-AS2 may act in a coordinated manner in breast cancer progression.

Further, functional enrichment analysis of the ncPath database (Figure 8) also revealed common signaling pathways involving miR-106a-5p, miR-17-5p, and ADAMTS9-AS2. Moreover, TCF7L2 transcription factor involved in the Wnt and Hippo signaling pathways and focal adhesion, may be suggest as a shared target of the studied miRNAs and ADAMTS9-AS2. To explore the potential direct interaction between lncRNA ADAMTS9-AS2 and TCF7L2, we analyzed the LncRRISearch database, which predicted five possible binding sites with a total energy of local base pair interactions of -68.91 kcal/mol. Similarly, the miRWalk 2.0 database indicated potential direct interactions between TCF7L2 and miR-106a-5p/miR-17-5p, suggesting that these miRNAs may bind to the 3'-UTR of TCF7L2. Based on these in silico results, it is plausible that ADAMTS9-AS2 could function as a competitive endogenous RNA (ceRNA), sequestering miR-106a-5p and miR-17-5p, thereby preventing their interaction with TCF7L2.

A review of the literature in the PubMed database revealed no existing studies on the role of ADAMTS9-AS2 and miR-106a-5p/miR-17-5p in regulating TCF7L2 within the Hippo and Wnt signaling pathways and cell adhesion in breast cancer, further emphasizing the novelty and relevance of our findings. Although our current study is based on bioinformatic and correlation analyses, future *in vitro* validation, such as dual-luciferase assays, knockdown/overexpression, and miRNA mimic/inhibitor experiments, is necessary to confirm the functional relevance of the proposed ADAMTS9-AS2/miR-17-5p (miR-106a-5p)/TCF7L2 axis.

Based on bioinformatic predictions, the experimental data, and literature review, we constructed a regulatory network that reflects potential interactions between the investigated long non-coding RNAs (ADAMTS9-AS2, HAND2-AS1, HOTAIRM1, MEG3), microRNAs (miR-17-5p, miR-106a-5p, and others), the key DNA methyltransferase DNMT1, and genes associated with epithelial-mesenchymal transition (EMT) and metastasis (such as TCF7L2, VIM, VEGFA, ZEB1, CDH1, PTEN, TGFB1) in the context of breast cancer (Figure 9). Notably, the identified connections between miR-17-5p, miR-106a-5p, and DNMT1 suggest that these miRNAs may influence the epigenetic regulation of DNA methylation, potentially affecting the expression of other genes in the regulatory network, including lncRNAs and EMT-related genes, thereby contributing to the complex landscape of tumor progression.

DISCUSSION

The observed synergy between changes in gene expression and/or methylation levels strongly supports the hypothesis of potential joint functions of the investigated lncRNAs. Utilizing a robust combination of bioinformatic methods with experimental validation through RT-qPCR and MS-qPCR, we have established highly significant pairwise co-expression and co-methylation among several lncRNAs implicated in the regulation of key signaling pathways in breast cancer. Importantly, we report for the first time specific co-expressed lncRNA pairs – MEG3–HOTAIRM1, MEG3–ADAMTS9-AS2, MEG3–HAND2-AS1 – and co-methylated pairs – HAND2-AS1–ADAMTS9-AS2, MEG3–HAND2-AS1, HOTAIRM1–ADAMTS9-AS2 – in breast cancer, with consistent support from the GEPIA 2.0 database. These converging results across our experimental data and a large-scale independent dataset reinforce the hypothesis of functional coordination among these lncRNA pairs.

The growing number of studies on lncRNA interactions in cancer biology highlights this as a highly relevant and rapidly evolving area. For example, lncRNA PSMG3-AS1 and MEG3 have

been shown to negatively regulate each other, affecting proliferation in endometrial carcinoma cells [18], while lncRNA POU3F3 promotes melanoma cell proliferation by suppressing MEG3 [19]. Similarly, HLA-F-AS1 binds MEG3 in glioblastoma, promoting invasion and migration while inhibiting apoptosis [20]. HAND2-AS1 has also been shown to be suppressed by lncRNA WTAPP1 in non-small cell lung cancer, thereby enhancing invasion and migration [21]. To date, however, no studies have investigated the interplay among ADAMTS9-AS2, HAND2-AS1, HOTAIRM1, and MEG3 specifically in breast cancer. The positive expression correlations we identified suggest a possible synergistic role in regulating shared signaling pathways, representing a novel insight into coordinated lncRNA expression patterns in this disease.

Functional enrichment analysis using the NcPath database revealed potential involvement of both miRNAs (miR-106a-5p and miR-17-5p) and lncRNAs (ADAMTS9-AS2, HAND2-AS1, HOTAIRM1, MEG3) in breast cancer-related signaling pathways, a finding also supported by evidence from other tumor types. Multiple studies have implicated these lncRNAs in the PI3K signaling pathway. For example, MEG3 downregulation is observed in retinoblastoma and breast cancer cells, whereas its overexpression suppresses cell proliferation and inactivates the PI3K/Akt/mTOR pathway, thereby reducing migration and enhancing apoptosis [22, 23]. Similarly, ADAMTS9-AS2 inhibits the PI3K/AKT/mTOR pathway in liver cancer by upregulating ADAMTS9, promoting autophagy, and suppressing migration and invasion [24]. In salivary gland adenoid cystic carcinoma, elevated ADAMTS9-AS2 expression reduces ITGA6 levels via miR-143-3p, indirectly affecting the PI3K/Akt and MEK/Erk pathways [25]. HOTAIRM1 has been shown to suppress the PI3K/AKT pathway in gastric cancer by sponging miR-17-5p, leading to increased PTEN expression [26]. HAND2-AS1 also inhibits proliferation in non-small-cell lung cancer via the PI3K/Akt pathway [27].

Based on literature analysis, we identified MEG3 and HOTAIRM1 as inhibitors of the Wnt/ β -catenin pathway in oral squamous cell carcinoma, melanoma, and hepatocellular carcinoma [28–30], suggesting a broader tumor-suppressive role. The convergence of these literature findings with our bioinformatic predictions points to a likely involvement of these lncRNAs in similar signaling cascades in breast cancer. While our observations are based on correlative data and may include indirect regulatory effects, they align well with previously published results in other cancer types and provide a solid foundation for future functional investigations specifically focused on breast cancer.

Our assumption regarding the cooperative involvement of the studied lncRNAs in key signaling pathways and biological processes in breast cancer, based on the observed co-expression and co-methylation patterns, is supported by existing literature, albeit predominantly in cancers of other origins. Notably, to date, only one study has examined the role of any of the investigated lncRNAs in the relevant signaling pathways specifically in breast cancer [23], emphasizing the novelty and potential significance of our broader analysis.

In this context, we were the first to identify a moderate negative correlation between miR-106a-5p and ADAMTS9-AS2 ($r_s = -0.46$; $p = 0.03$), as well as between miR-17-5p and ADAMTS9-AS2 ($r_s = -0.41$; $p = 0.04$), suggesting the possibility of direct or indirect regulatory interactions. Supporting this, the DIANA-LncBase v3 database predicts a potential direct binding between ADAMTS9-AS2 and miR-106a-5p. Additionally, bioinformatic analysis revealed that TCF7L2—a gene implicated in Wnt and Hippo signaling as well as focal adhesion—may represent a common downstream target of these miRNAs and ADAMTS9-AS2. Although the sample size of 50 may limit the statistical power to detect subtle correlations, we plan to expand the cohort size in future studies to improve the reliability of these findings.

These novel correlations and predicted molecular interactions highlight candidate regulatory axes that could play a role in breast cancer biology and provide a strong conceptual framework for further functional studies aimed at elucidating their mechanistic relevance.

Our analysis using LncRRIsearch and miRWalk 2.0 revealed at least five potential binding sites for miR-106a-5p and miR-17-5p in ADAMTS9-AS2 and in the 3'-UTR of TCF7L2, supporting the possibility of direct molecular interactions among these components.

A PubMed literature search yielded no reports on the involvement of ADAMTS9-AS2 and miR-106a-5p/miR-17-5p in regulating TCF7L2 within the Wnt or Hippo pathways or in cell adhesion in breast cancer, highlighting the originality of our findings and their potential to identify novel targets for intervention.

A previous study [31] demonstrated that ADAMTS9-AS2 can regulate MEG3 by acting as a molecular sponge for miR-106a-5p in non-invasive bladder cancer. Our findings suggest that a similar regulatory interaction may be present in breast cancer, implying that the ADAMTS9-AS2–MEG3 axis could represent a conserved mechanism across different tumor types. This potential cross-cancer conservation underscores the biological relevance of this regulatory pathway and highlights its broader significance in cancer biology.

Although direct therapeutic applications have yet to be established, our findings provide a valuable basis for understanding potential regulatory interactions involved in breast cancer. Further studies are necessary to evaluate the feasibility of targeting these mechanisms using existing pharmacological agents or RNA-based therapeutics. Nevertheless, the identified lncRNA–miRNA–mRNA networks may represent promising directions for future translational research and the development of targeted intervention strategies.

CONCLUSION

An integrated approach combining bioinformatic analysis with experimental validation revealed coordinated changes in the expression and methylation of four lncRNAs—: MEG3, ADAMTS9-AS2, HAND2-AS1, and HOTAIRM1—, as well as miRNAs miR-106a-5p and miR-17-5p, suggesting their potential mutual regulation. The observed co-expression and co-methylation patterns point to possible functional cooperation among these molecules, supported by the identification of shared signaling pathways, including the Hippo, MAPK, and Wnt pathways, as well as pathways related to adherens junctions and focal adhesion.

Novel interactions were identified between ADAMTS9-AS2 and miR-106a-5p/miR-17-5p, with TCF7L2 predicted as a common downstream target. These results, supported by both experimental data and bioinformatic predictions, suggest the involvement of a competitive endogenous RNA (ceRNA) mechanism within the ADAMTS9-AS2 – miR-106a-5p/miR-17-5p – TCF7L2 regulatory axis. Computational analysis of binding energies also indicates a potential for direct binding between these miRNAs and both ADAMTS9-AS2 and TCF7L2 mRNA, though this requires further experimental confirmation.

Altogether, the identification of novel co-regulated lncRNAs and miRNAs in this study contributes to a better understanding of regulatory networks in breast cancer and may inform the development of new therapeutic strategies. Characterizing lncRNA–miRNA–mRNA interactions represent a promising direction for future research into targeted interventions.

ACKNOWLEDGMENTS

The authors express their gratitude to the staff of Blokhin National Medical Research Center of Oncology for their assistance in selecting a collection of breast cancer tissue samples.

Conflicts of interest: Authors declare no conflicts of interest.

Funding: This work was supported by the Russian Science Foundation grant no. 24-75-00159.

Data availability: The data presented in this study are available on reasonable request from the corresponding author.

Submitted: 05 March 2025

Accepted: 05 May 2025

Published online: 09 May 2025

REFERENCES

1. Bray F, Laversanne M, Sung H, Ferlay J, Siegel RL, Soerjomataram I, et al. Global cancer statistics 2022: GLOBOCAN estimates of incidence and mortality worldwide for 36 cancers in 185 countries. *CA Cancer J Clin.* 2024; 74: 229-263; doi: 10.3322/caac.21834
2. Steeg P.S. Targeting metastasis. *Nat Rev Cancer.* 2016; 16: 201-18; doi: 10.1038/nrc.2016.25
3. Yan X., Hu Z., Feng Y. et al. Comprehensive genomic characterization of long non-coding RNAs across human cancers. *Cancer Cell.* 2015; 28: 529–540; doi: 10.1016/j.ccell.2015.09.006
4. Peinado P., Herrera A., Baliñas C., Martín-Padrón J., Boyero L., Cuadros M., et al. Long noncoding RNAs as cancer biomarkers. *Cancer Noncoding RNAs.* 2018; 95-114; doi:10.1016/B978-0-12-811022-5.00006-1
5. Slaby O., Laga R., Sedlacek O. Therapeutic targeting of non-coding RNAs in cancer. *Biochem J.* 2017; 474: 4219–4251; doi: 10.1042/BCJ20170079
6. Swellam M., el Magdoub H.M., Shawki M.A. et al. Clinical impact of LncRNA XIST and LncRNA NEAT1 for diagnosis of high-risk group breast cancer patients. *Curr Probl Cancer.* 2021; 455: 100709; doi: 10.1016/j.currprobcancer.2021.100709

-
7. Li X., Dai A., Tran R., Wang J. Identifying miRNA biomarkers for breast cancer and ovarian cancer: a text mining perspective. *Breast Cancer Res Treat.* 2023; 201: 5-14; doi: 10.1007/s10549-023-06996-y
 8. Bartel D.P. MicroRNAs: genomics, biogenesis, mechanism, and function. *Cell.* 2004; 116: 281–297; doi: 10.1016/s0092-8674(04)00045-5
 9. López-Urrutia E., Bustamante Montes L.P., Ladrón de Guevara Cervantes D., Pérez-Plasencia C., Campos-Parra A.D. Crosstalk Between Long Non-coding RNAs, MicroRNAs and mRNAs: Deciphering Molecular Mechanisms of Master Regulators in Cancer. *Front Oncol.* 2019; 25: 669; doi: 10.3389/fonc.2019.00669
 10. Li R., Xu H., Gao X. The ceRNA network regulates epithelial-mesenchymal transition in colorectal cancer. *Heliyon.* 2023; 9, e14143; doi: 10.1016/j.heliyon.2023.e14143
 11. Yan H., Bu P. Non-coding RNA in cancer. *Essays Biochem.* 2021; 65: 625-639; doi: 10.1042/EBC20200032
 12. Lukina S.S., Burdenny A.M., Filippova E.A., Pronina I.V., Ivanova N.A., Kazubskaya T.P., Kushlinskii D.N., Utkin D.O., Loginov V.I., Braga E.A., Kushlinskii N.E. Synergy between the Levels of Methylation of microRNA Gene Sets in Primary Tumors and Metastases of Ovarian Cancer Patients. *Bull Exp Biol Med.* 2022; 173: 87-91; doi: 10.1007/s10517-022-05499-y
 13. Pronina I., Lukina S., Loginov V., Burdenny A., Kazubskaya T, Braga E., Filippova E. Experimental Identification of Aberrantly Expressed Long Non-Coding RNAs in Breast Cancer. *Med. Sci. Forum.* 2023; 21: 7; doi.org/10.3390/ECB2023-14083

-
14. TNM Classification of Malignant Tumours. Eds.: Brierley J.D, Gospodarowicz M.K., Wittekind C.. Chichester, West Sussex, UK; Hoboken, NJ: John Wiley & Sons, 2017
 15. World Medical Association. World Medical Association Declaration of Helsinki: ethical principles for medical research involving human subjects. *JAMA*. 2013; 310: 2191-2194
 16. Loginov V.I., Pronina I.V., Filippova E.A., Burdenny A.M., Lukina S.S., Kazubskaya T.P., et al. Aberrant methylation of 20 miRNA genes specifically involved in various steps of ovarian carcinoma spread: from primary tumors to peritoneal macroscopic metastases. *Int. J. Mol. Sci.* 2022; 23: 1300; doi: 10.3390/ijms23031300
 17. Livak K.J., Schmittgen T.D. Analysis of relative gene expression data using real-time quantitative PCR and the $2^{-\Delta\Delta CT}$ method. *Methods*. 2001, 25, 402-408; doi: 10.1006/meth.2001.1262
 18. Huang S., Chen J., Gao X., Shang Z., Ma X., Zhang X., Li J., Yin R., Meng X. LncRNAs PSMG3-AS1 and MEG3 negatively regulate each other to participate in endometrial carcinoma cell proliferation. *Mamm Genome*. 2022, 33, 502-507; doi: 10.1007/s00335-021-09931-y
 19. Liu Y., Zhuang Y., Fu X., Li C. LncRNA POU3F3 promotes melanoma cell proliferation by downregulating lncRNA MEG3. *Discov Oncol*. 2021, 12, 21; doi: 10.1007/s12672-021-00414-9
 20. Wang Y., Xie T., Liu H., Yu X. LncRNA HLA-F-AS1 Enhances the Migration, Invasion and Apoptosis of Glioblastoma Cells by Targeting lncRNA MEG3. *Cancer Manag Res*. 2021, 13, 9139-9145; doi: 10.2147/CMAR.S322351

-
21. Zhang L., Jin C., Yang G., Wang B., Hua P., Zhang Y. LncRNA WTAPP1 promotes cancer cell invasion and migration in NSCLC by downregulating lncRNA HAND2-AS1. *BMC Pulm Med.* 2020, 20, 153; doi: 10.1186/s12890-020-01180-0.
 22. Yan X., Jia H., Zhao J. LncRNA MEG3 attenuates the malignancy of retinoblastoma cells through inactivating PI3K /Akt/mTOR signaling pathway. *Exp Eye Res.* 2023, 226, 109340; doi:10.1016/j.exer.2022.109340
 23. Zhu M., Wang X., Gu Y., Wang F., Li L., Qiu X. MEG3 overexpression inhibits the tumorigenesis of breast cancer by downregulating miR-21 through the PI3K/Akt pathway. *Arch Biochem Biophys.* 2019, 661, 22-30; doi: 10.1016/j.abb.2018.10.021
 24. Li H., Huang H., Li S., Mei H., Cao T., Lu Q. Long non-coding RNA ADAMTS9-AS2 inhibits liver cancer cell proliferation, migration and invasion. *Exp Ther Med.* 2021, 21, 559; doi:10.3892/etm.2021.9991
 25. Xie S., Yu X., Li Y., Ma H., Fan S., Chen W., Pan G., Wang W., Zhang H., Li J., Lin Z. Upregulation of lncRNA ADAMTS9-AS2 Promotes Salivary Adenoid Cystic Carcinoma Metastasis via PI3K/Akt and MEK/Erk Signaling. *Mol Ther.* 2018, 26, 2766-2778; doi: 10.1016/j.ymthe.2018.08.018
 26. Lu R., Zhao G., Yang Y., Jiang Z., Cai J., Zhang Z., Hu H. Long noncoding RNA HOTAIRM1 inhibits cell progression by regulating miR-17-5p/ PTEN axis in gastric cancer. *J Cell Biochem.* 2019, 120, 4952-4965; doi: 10.1002/jcb.27770
 27. Gao T., Dai X., Jiang Y., He X., Yuan S., Zhao P. LncRNA HAND2-AS1 inhibits proliferation and promotes apoptosis of non-small cell lung cancer cells by inactivating PI3K/Akt pathway. *Biosci Rep.* 2020, 40, BSR20201870; doi: 10.1042/BSR20201870

-
28. Liu Z., Wu C., Xie N., Wang P. Long non-coding RNA MEG3 inhibits the proliferation and metastasis of oral squamous cell carcinoma by regulating the WNT/ β -catenin signaling pathway. *Oncol Lett.* 2017, 14, 4053-4058; doi: 10.3892/ol.2017.6682
29. Li P., Gao Y., Li J., Zhou Y., Yuan J., Guan H., Yao P. LncRNA MEG3 repressed malignant melanoma progression via inactivating Wnt signaling pathway. *J Cell Biochem.* 2018, 119, 7498-7505; doi: 10.1002/jcb.27061
30. Zhang Y., Mi L., Xuan Y., Gao C., Wang Y.H., Ming H.X., Liu J. LncRNA HOTAIRM1 inhibits the progression of hepatocellular carcinoma by inhibiting the Wnt signaling pathway. *Eur Rev Med Pharmacol Sci.* 2018, 22, 4861-4868; doi: 10.26355/eurrev_201808_15622
31. Kouhsar M., Azimzadeh Jamalkandi S., Moeini A., Masoudi-Nejad A. Detection of novel biomarkers for early detection of Non-Muscle-Invasive Bladder Cancer using Competing Endogenous RNA network analysis. *Sci Rep.* 2019, 9, 8434; doi: 10.1038/s41598-019-44944-3
32. Hattermann K., Mehdorn H.M., Mentlein R., Schultka S., Held-Feindt J. A methylation-specific and SYBR-green-based quantitative polymerase chain reaction technique for O6-methylguanine DNA methyltransferase promoter methylation analysis. *Anal. Biochem.* 2008; 377: 62-71; doi: 10.1016/j.ab.2008.03.014
33. Chen Z., Bian C., Huang J., Li X., Chen L., Xie X., Xia Y., Yin R., Wang J. Tumor-derived exosomal HOTAIRM1 regulates SPON2 in CAFs to promote progression of lung adenocarcinoma. *Discov Oncol.* 2022; 13: 92; doi: 10.1007/s12672-022-00553-7
34. Loginov V.I., Dmitriev A.A., Senchenko V.N., Pronina I.V., Khodyrev D.S., Kudryavtseva A.V., et al. Tumor Suppressor Function of the SEMA3B Gene in

TABLES AND FIGURES WITH LEGENDS

Table 1. Clinical and pathomorphological parameters of samples from breast cancer patients.

Clinical and histological parameter		Number of samples for expression studies N=50	Number of samples for methylation studies N=127
Stage	I + II	44	96
	III	6	31
Tumor size	T1	14	30
	T2	29	77
	T3	3	10
	T4	4	9
Lymphnode metastases	Yes	21	62
	No	29	65
Molecular subtype*	Basal	1	7
	Erb-B2	3	12
	Luminal A	6	16
	Luminal B	37	82
Receptor expression*	ER+/ER-	43/4	94/23
	PR+/PR-	40/7	88/29
	HER2+/HER2-	24/23	62/55
Grade*	G1	8	16
	G2	33	87

	G3	6	22
--	----	---	----

* Note: Clinical or molecular data were unavailable for some samples; therefore, the total number of cases may vary between parameters.

Table 2. Primer nucleotide sequences and MS-qPCR parameters.

Gene	Primers for MS-qPCR*, 5'→3'	T _{ann} , °C	PCR product, bp
ADAMTS9-AS	MF: AATTTTCGATAGCGTATTTTCGGGAGTTAC	59	187
	MR: TCTTAAAATTCCCAAACACATCCTTCCT		
	UF: TTTTGATAGTGTATTTTGGGAGTTATGG	56	238
	UR: AATACTCACCCCAAACACTAAACTACT		
HAND2-AS1	MF: CGAGGTTGGTACGCGGAG	60	121
	MR: CCGACACA ACTAAACCGACTC		
	UF: TGGGGTTTTTGTGAGGTTGGTATGT	60	134
	UR: CCCCAACACA ACTAAACCAACTCCTC		
HOTAIRM1	MF: TTTAGGCGGCGGTAGTTGTTGC	60	212
	MR: ACCCTCTCCCTTCTCACCTCTCG		
	UF: GATTTGGAGTGTGGAGTGAAGAAGA	60	219
	UR: TTACAACCACCCAACA AACTCTAACC		
MEG3	MF: CGTAAAGTTCGTATTTTTCGATGGATGTT	60	185
	MR: CGCGAATACTTTTTCCCTACGTAAACC		
	UF: TGATGGATGTTTTGAAATTGTTAGGTGTG	60	165
	UR: CAAATACTTTTTCCCTACATAAACCCTCA		
ACTB1**	BSF: TGGTGATGGAGGAGGTTTAGTAAGT	60	135
	BSR: AACCAATAAAACCTACTCCTCCCTTAA		

Note: MF/UF is a forward primer for a methylated/unmethylated allele, MR/UR is a reverse primer for a methylated/unmethylated allele. BS – primers for bisulfite-converted DNA *All oligonucleotides were selected using the SeqBuilder Pro program, which is included in the Lasergene 17.1 software package from DNASTAR, Madison, WI, USA. **Taken from [32].

Table 3. Primer nucleotide sequences and RT-qPCR parameters.

Gene	Primers for RT-qPCR*, 5'→3'	T _{ann} , °C	PCR product, bp
ADAMTS9-AS2	F: CTCCACCCGATCCTTCCATTGA	57.9	199
	R: GGGGGTCTTGCTCTTTCCTTATCC		
HAND2-AS1	F: CCCCGAATCTGTAGTGTGGC	59	113
	R: CAGGCGGTGGAGAGGACT		
HOTAIRM1**	F: AGGGGGTTGAAATGTGGGTG	60	162
	R: CTTGAAAGTGGAGAAATAAAGTGCC		
MEG3	F: CGGCTGGGTCGGCTGAAGAACT	59	208
	R: CCGTGGCTGTGGAGGGATTT		
B2M***	F: TGACTTTGTCACAGCCCAAGATAG	64	81
	R: CAAATGCGGCATCTTCAAACCTC		

*Note: F – forward primer; R – reverse primer. Primers were selected using the SeqBuilder Pro program, which is included in the Lasergene 17.1 software package from DNASTAR, Madison, WI, USA. ** Taken from [33], *** Taken from [34].

Table 4. Spearman's correlation coefficient values for coexpressed and comethylated lncRNA pairs according to data of RT-qPCR in cohort of 50 breast cancer specimens.

lncRNA pairs	co-expression* lncRNA (r _s); p<0.05	co-expression (GEPIA) lncRNA (r _s);	co-methylation* lncRNA (rs) p<0.001

		p<0.001	
MEG3 – HOTAIRM1	0.47	0.57	
MEG3 – ADAMTS9-AS2	0.49	0.58	
MEG3 – HAND2-AS1	0.52	0.64	0.53
HAND2-AS1 – ADAMTS9-AS2		0.66	0.70
HAND2-AS1 – HOTAIRM1		0.46	0.43
HOTAIRM1 – ADAMTS9-AS2		0.49	0.52

* Note: co-expression/co-methylation experimentally obtained

Table 5. Characteristics of miR-17-5p and miR-106a-5p in breast cancer according to bioinformatic data bases

Feature Data	miR-17-5p	miR-106a-5p	Source(s)
Expression Level (Tumor vs. Normal)	Upregulation (FC = 2.38, p = 1.0e-8)	Upregulation (FC = 2.29, p = 2.7e-8)	TCGA-BRCA
Expression Validation	Corroborated (adjusted p < 0.05)		GEO: GSE22820
Clinical Correlation	Correlated with Stage (p = 2.28e-2), Lymph Node Involvement (p = 4.43e-4)	Strongly Correlated with Distant Metastasis (p = 1.88e- 6)	OncoMir, TCGA
Key Processes Involved	Proliferation, Invasion, Metastasis, EMT, Angiogenesis, Therapy Resistance		Literature Review

Major Target Genes	PTEN, E2F1, ZEB1		Literature Review
Enriched Signaling Pathways	"Pathways in cancer", MAPK signaling, Wnt signaling, Adherens junctions, Focal adhesion, Actin cytoskeleton regulation, Cell cycle control		Target Gene Functional Analysis
Validated Target Genes (EMT/Metastasis)	VEGFA, TGFBR2, TCF7L2	VEGFA, TGFBR2, TIMP2, HMGA2, TCF7L2	TarBase (Validated Data)

EARLY ACCESS

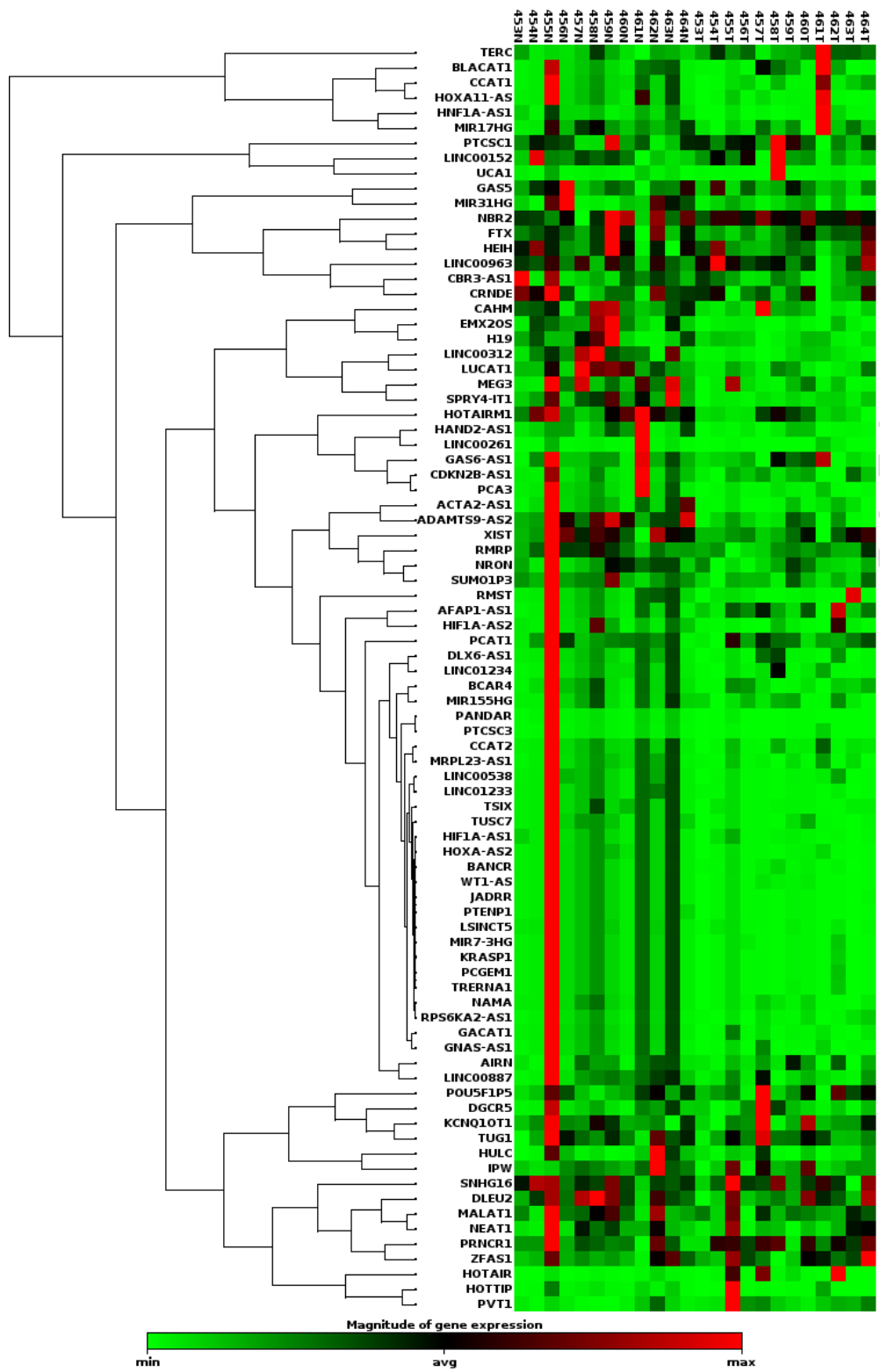


Figure 1. Differential expression of lncRNAs in 12 paired breast cancer specimens, obtained using the RT² lncRNA PCR Array Gene Expression Analysis kit; lncRNAs with fold change > 2 and *p*-value < 0.05 were considered statistically significant.

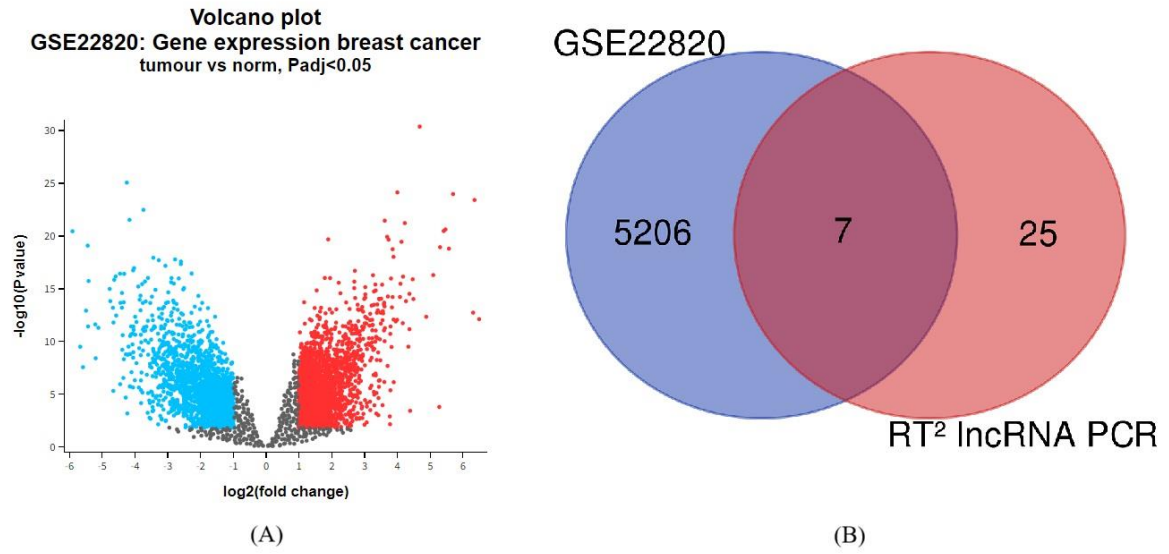


Figure 2. (A) Volcano plot of differentially expressed genes in the GSE22820 data set; (B) Venn diagram of differentially expressed genes in the GSE22820 dataset and those obtained by us experimentally.

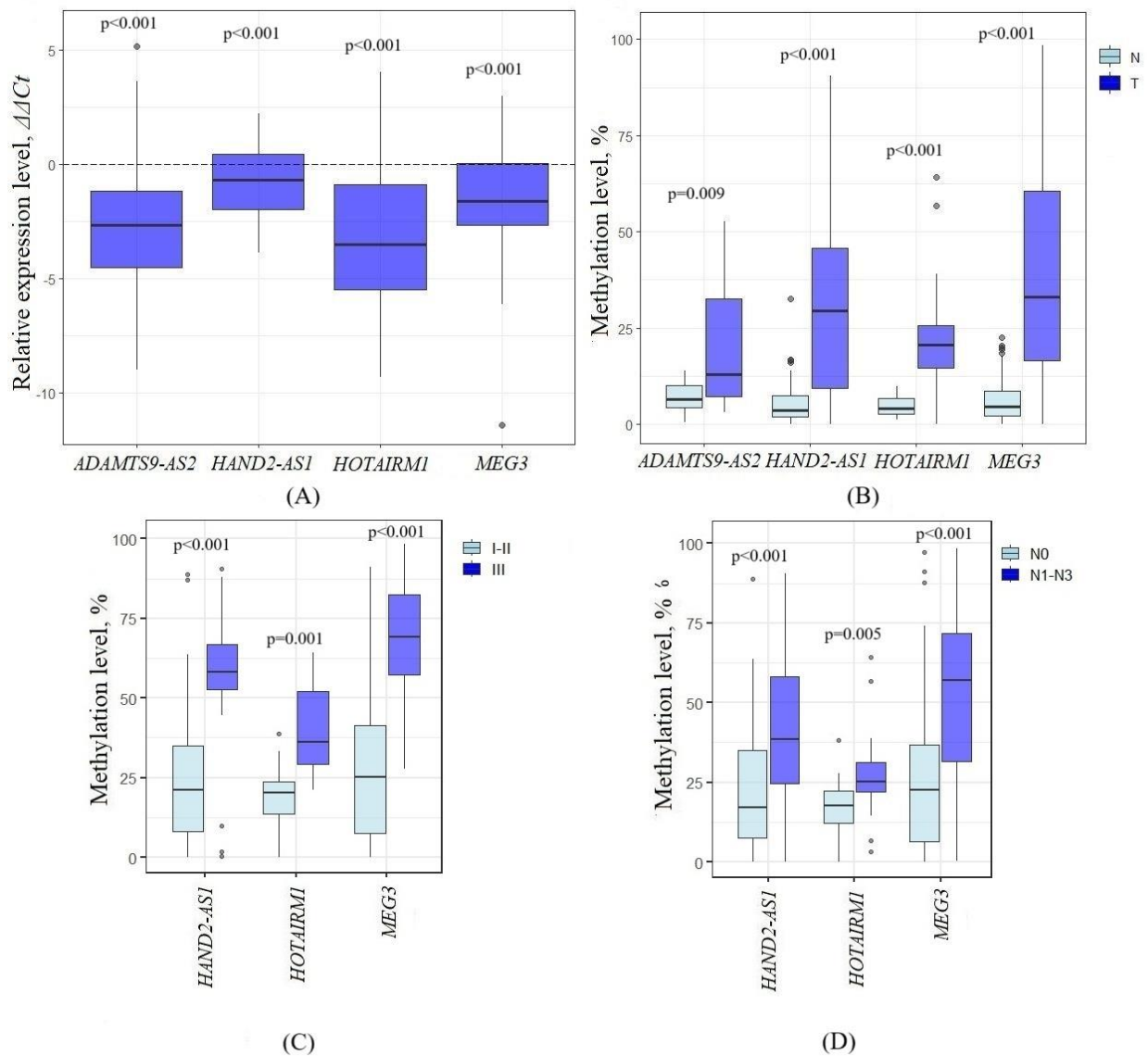


Figure 3. Expression and promoter methylation of candidate lncRNAs in breast cancer and their clinical relevance. (A) Expression profile of lncRNAs ADAMTS9-AS2, HOTAIRM1, MEG3, HAND2-AS1 in 50 breast tumor samples (B) Promoter methylation level of lncRNAs ADAMTS9-AS2, HOTAIRM1, MEG3, HAND2-AS1 in 127 breast tumor samples and in paired normal samples. (C) Association between lncRNA promoter methylation and breast cancer stage (I+II vs. III). (D) Association between lncRNA promoter methylation and lymphnode metastases status (N0 vs. N1–N3). Statistical significance was assessed using the Mann–Whitney U test.

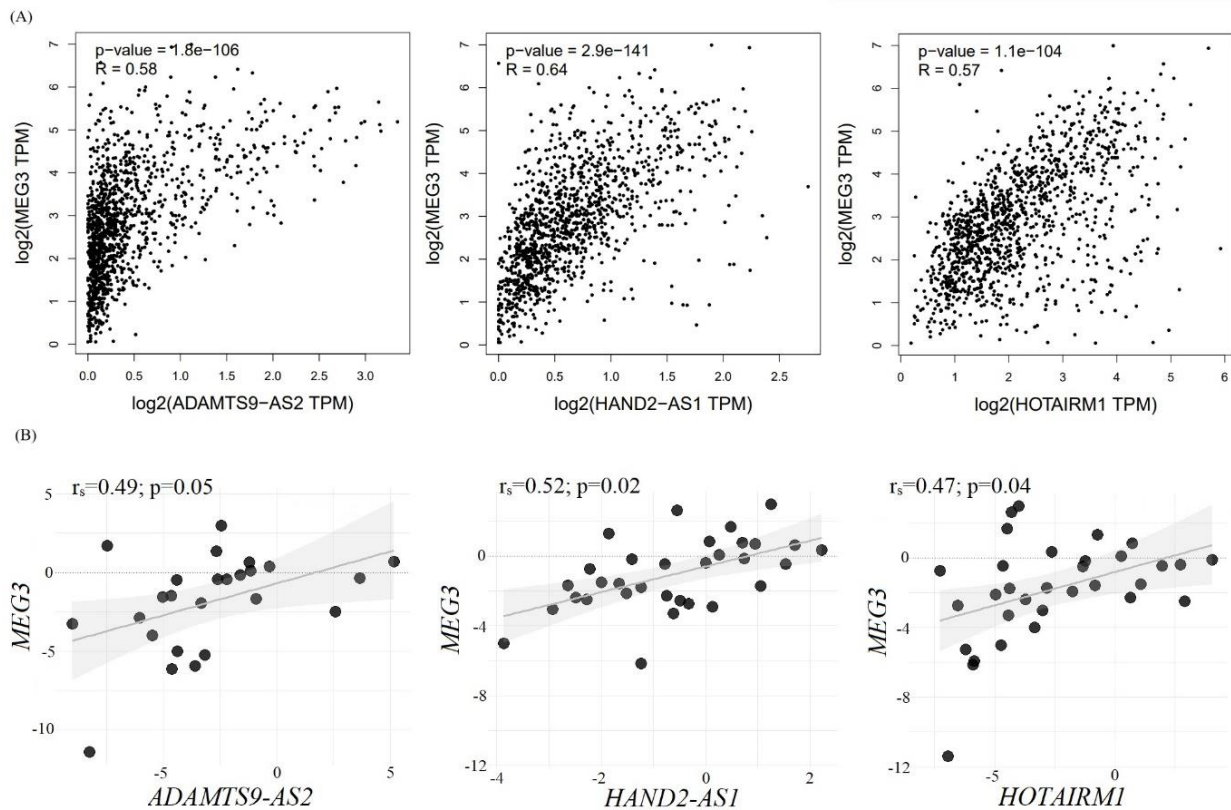


Figure 4. Correlation of relative expression levels of lncRNAs MEG3-ADAMTS9-AS2, MEG3-HAND2-AS1, MEG3-HOTAIRM1: (A) according to TCGA data (built in GEPIA 2.0); (B) according to experimental data. 50 paired breast cancer samples were examined.

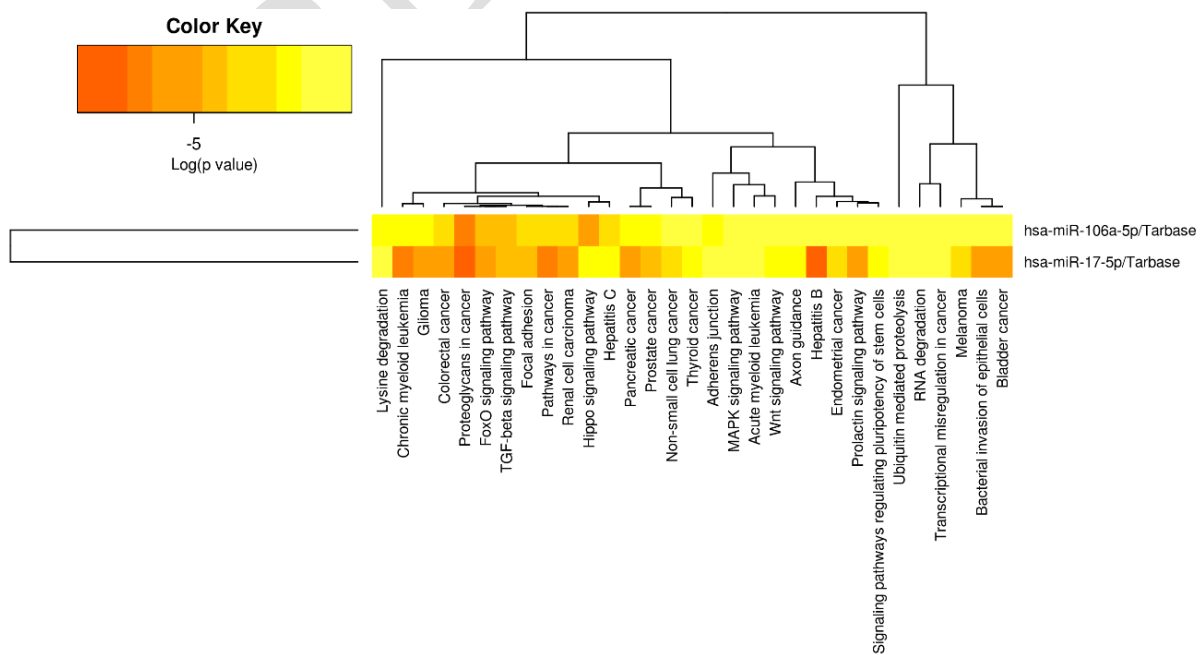


Figure 5. Heatmap reflecting the signaling pathways in which miRNAs miR-106a-5p and miR-17-5p are involved.

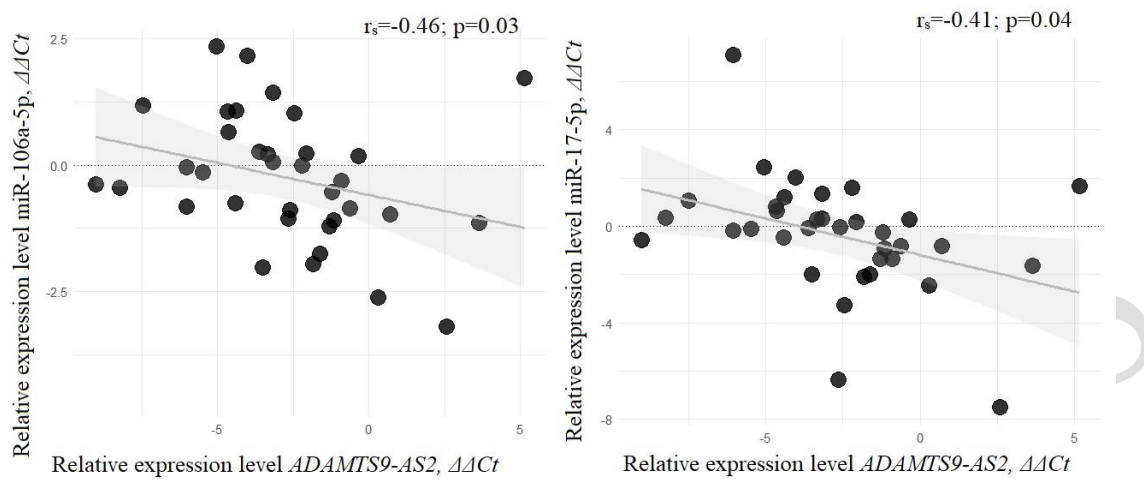


Figure 6. Correlation of relative expression levels of lncRNA ADAMTS9-AS2 and miRNAs miR-17-5p and miR-106a-5p; 50 paired breast cancer samples were examined.

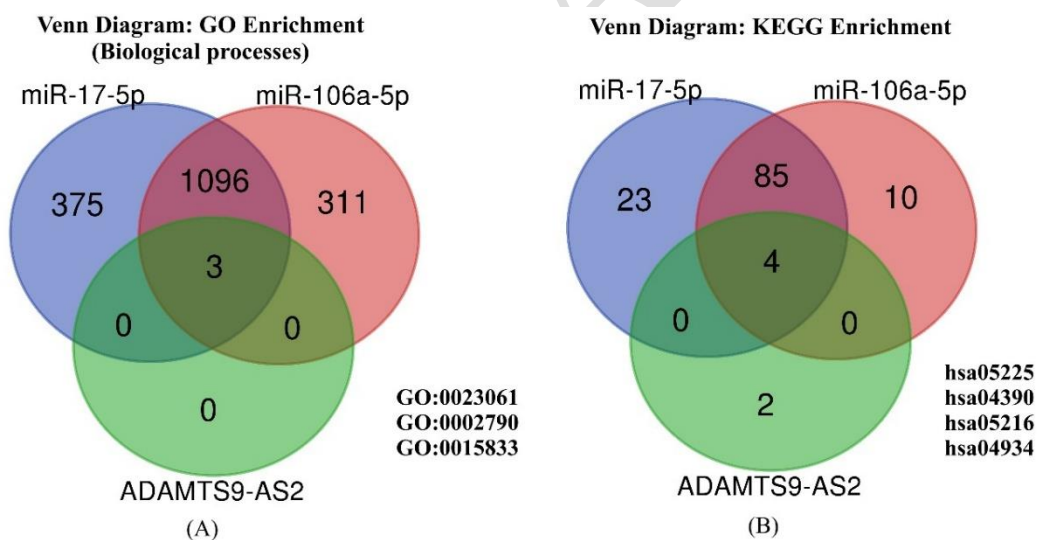


Figure 7. Intersection of functional enrichment results. (A) Venn diagram shows the overlapping Gene Ontology (GO) biological processes for miR-17-5p, miR-106a-5p, and ADAMTS9-AS2. (B) Venn diagram shows the overlapping KEGG signaling pathways for miR-17-5p, miR-106a-5p, and ADAMTS9-AS2.

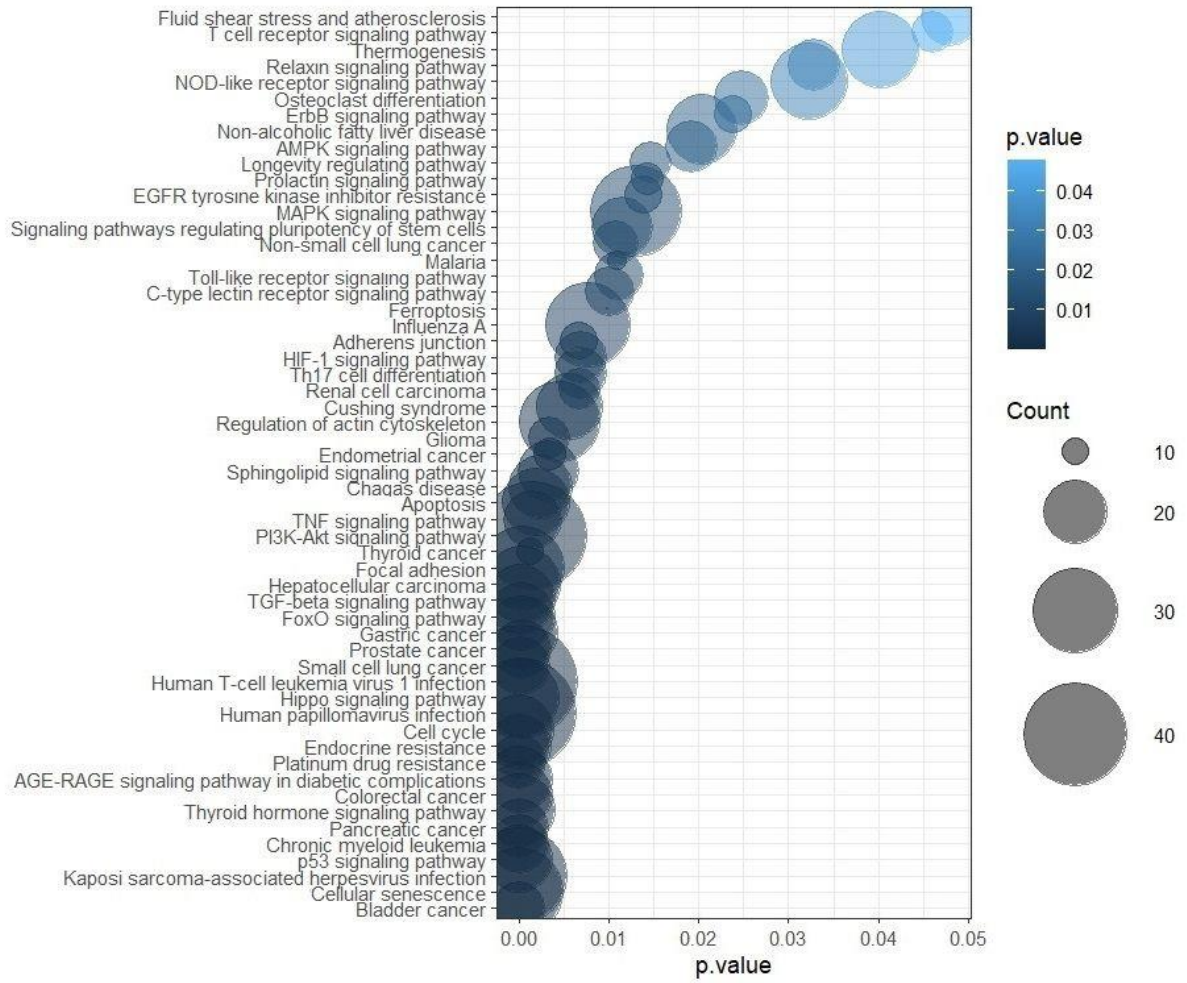


Figure 8. Results of functional enrichment analysis of the ncPath database involving miRNAs (miR-106a-5p and miR-17-5p) and lncRNA ADAMTS9-AS2.

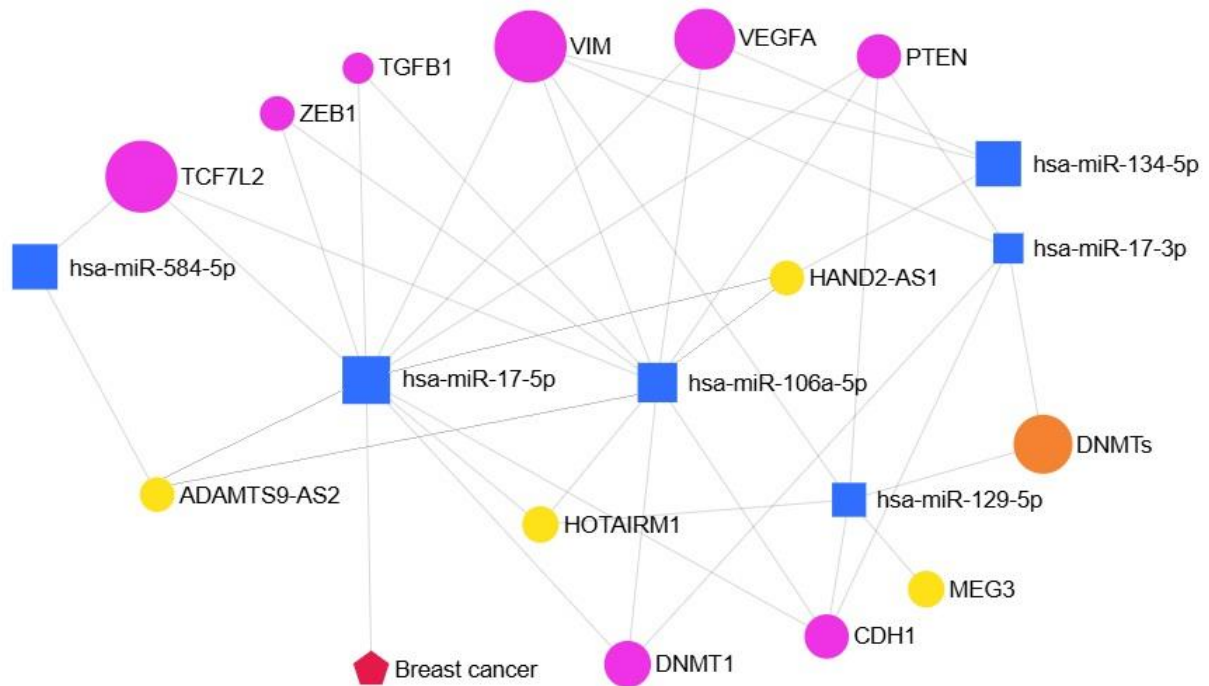


Figure 9. Regulatory network highlighting potential interactions between lncRNAs, miRNAs, DNMTs, and EMT-related genes in breast cancer. Yellow circles: lncRNAs; blue squares: miRNAs; orange circle: DNMTs; magenta circles: EMT/metastasis genes; red pentagon: Breast cancer. Lines indicate potential regulatory relationships.

SUPPLEMENTAL DATA

Table S1. Fold change and p-value of differentially expressed of lncRNAs obtained using the RT² lncRNA PCR Array Gene Expression Analysis kit in breast cancer.

N ^o	Gene	FC	p-value
1	ACTA2-AS1	-4.25	0.02
2	ADAMTS9-AS2	-7.21	<0.001
3	BANCR	-4.88	0.04
4	EMX2OS	-13.2	<0.001

N ^o	Gene	FC	p-value
17	MEG3	-4.56	0.04
18	MIR31HG	-2.87	0.04
19	MIR7-3HG	-5.56	0.04
20	NAMA	-4.85	0.04

5	H19	-2.94	0.02
6	HAND2-AS1	-6.91	0.03
7	HIF1A-AS1	-5.14	0.04
8	HOTAIRM1	-3.67	<0.001
9	HOXA-AS2	-6.46	0.03
10	JADRR	-6.92	0.03
11	KRASPI	-6.06	0.04
12	LINC00312	-7.83	<0.001
13	LINC00538	-5.85	0.04
14	LINC01233	-6.62	0.02
15	LSINCT5	-5.66	0.03
16	LUCAT1	-4.57	<0.001

21	PCA3	-5.84	0.05
22	PCGEM1	-5.94	0.04
23	PTENP1	-7.68	0.03
24	RMRP	-1.68	0.04
25	SPRY4-IT1	-5.14	<0.001
26	TERC	2.24	0.03
27	TRERNA1	-5.8	0.04
28	TSIX	-5.79	0.02
29	TUSC7	-6.37	0.03
30	WT1-AS	-5.7	0.04
31	XIST	-2.34	0.04
32	RPLP0	1.85	<0.001